HHS Public Access

Author manuscript

Pain. Author manuscript; available in PMC 2024 June 01.

Published in final edited form as:

Pain. 2023 June 01; 164(6): e274–e285. doi:10.1097/j.pain.0000000000002834.

AIBP regulates TRPV1 activation in CIPN by controlling lipid raft dynamics and proximity to TLR4 in DRG neurons

Juliana M. Navia-Pelaez[1], **Julia Borges Paes Lemes**[2], **Leonardo Gonzalez**[1], **Lauriane Delay**[2], **Luciano dos Santos Aggum Capettini**[1], **Jenny W. Lu**[1], **Gilson Gonçalves Dos Santos**[2], **Ann M. Gregus**[3], **Patrick M. Dougherty**[4], **Tony L. Yaksh**[2], **Yury I. Miller**[1,#]

[1]Department of Medicine, University of California, San Diego, La Jolla, California, USA;

[2]Department of Anesthesiology, University of California, San Diego, La Jolla, California, USA;

[3]School of Neuroscience, Virginia Polytechnic and State University, Blacksburg, Virginia, USA;

[4]Departments of Anesthesia and Pain Medicine, University of Texas MD Anderson Cancer Center, Houston, Texas, USA.

1. Introduction

Neuropathic pain remains a challenge for many cancer patients who receive chemotherapeutic treatment and who have limited and rarely effective options for pain management [24], underscoring the need for identifying novel therapeutic targets. Chemotherapy-induced peripheral neuropathy (CIPN) is characterized by enhanced peripheral nociceptive signaling that relies on the activation of ligand- and voltage-gated channels in dorsal horn and dorsal root ganglia [2;12;43], a property which positions each as a rational therapeutic target. Here we consider an alternative strategy by the selective targeting of lipid rafts associated with neuraxial cellular components known to regulate nociceptive processing.

Current work emphasizes that many of these receptors and channels mediating painful neuropathies are localized to and become activated in cholesterol-rich lipid raft membrane domains [34]. Depletion of cholesterol from the plasma membrane destabilizes these lipid rafts and serves to downregulate channel/receptor function [1;17;37;38]. In immune cells, including macrophages and microglia, ligand-dependent toll-like receptor 4 (TLR4) recruitment to lipid rafts is an initial step in the facilitatory cascade leading to TLR4 dimerization (activation) and lipid raft enlargement [27]. Studies with TLR4 knockout mice and with TLR4 pharmacological inhibitors demonstrate that neuraxial TLR4 activation is essential for development of CIPN [22;31;32]. Importantly, it appears likely that the effects of TLR4 activation may serve to enhance nociceptive afferent signaling through an

[#]Corresponding author: Yury I. Miller, University of California, San Diego, 9500 Gilman Drive, La Jolla, CA 92093, USA, +1-858-822-5771, yumiller@health.ucsd.edu.

Conflict of interest statement

Miller YI and Yaksh TL are inventors listed in patent applications related to the topic of this paper and scientific co-founders of Raft Pharmaceuticals LLC. The terms of this arrangement have been reviewed and approved by the University of California San Diego, in accordance with its conflict-of-interest policies. Other authors declare that they have no competing interests.

interaction with other channels/receptors. Thus, TLR4 and TRPV1 both localize to lipid rafts [34;36]. Current evidence suggests that TLR4 physically interacts with TRPV1 in non-neuronal cells [16;28] to potentiate the functionality of TRPV1 channels [8;19;29;41] by enhancing phosphorylation and suppression of its desensitization via internalization [3;25;28;33]. Recent work has demonstrated that TLR4, along with TRPV1, aside from their non-neuronal disposition are expressed in small nociceptive DRG neurons and their expression is upregulated in CIPN [19;22;29]. These observations led us to consider TLR4 expressing lipid rafts (TLR4-rafts) in DRG nociceptors as a potential therapeutic target in CIPN.

In recent work, we identified the apolipoprotein A-I binding protein (AIBP) as a protein that binds to TLR4 and augments cholesterol depletion selectively from cells with high surface expression of TLR4 [31;40]. This leads to a specific reduction in lipid raft content and inhibition of TLR4 homodimerization, the key step in initiating inflammatory signaling [6;40;44]. Intrathecal (i.t.) injection of AIBP reverses established tactile allodynia in CIPN mice [31;40].

Because TLR4 is highly expressed in small C-fibers and has been described to mediate paclitaxel-induced CIPN [19;22;29], we hypothesized that i.t. AIBP, via TLR4 binding, can target TLR4-rafts in DRG nociceptors. In this study, we found that paclitaxel-induced CIPN in mice is associated with increased lipid raft content, TLR4 surface expression, proximity of TRPV1 to TLR4, and TRPV1-induced increases in intracellular calcium in DRG neurons. All of these effects initiated by paclitaxel are enduringly reversed by i.t. AIBP. The AIBP ability to inhibit TRPV1 activation through a novel mechanism of disrupting TLR4-lipid rafts suggests its potential as a new treatment of CIPN neuropathic pain.

2. Methods

2.1. Animals

All animal experiments were approved by the Institutional Animal Care and Use Committees (IACUC) of the University of California, San Diego, Virginia Tech, and UT MD Anderson, and in accordance with the International Association for the Study of Pain (IASP) guidelines [30]. Eight-week old C57BL6/J mice were housed up to 4 per standard cage at room temperature and maintained on a 12:12 hour light/dark cycle with food and water *ad libitum*. All behavioral testing was performed by a blinded observer during the daylight cycle. Experiments were conducted in compliance with the US National Research Council's Guide for the Care and Use of Laboratory Animals [30].

2.1 CIPN model

To develop CIPN, intraperitoneal (i.p.) injections of paclitaxel (8 mg/kg/injection) were performed on days 1 and 3. Paclitaxel (Tocris Biosciences, 1097) was dissolved in a 1:1:8 mixture of ethanol, cremophor EL, and sterile 0.9% NaCl solution, respectively. In an alternative CIPN model, mice were injected on days 1 and 3 with 2.3mg/kg/injection of cisplatin (Spectrum Chemical MFG). Weight loss in excess of 20% body weight and

erratic behavior was considered the criteria for euthanasia; however, no animals required euthanasia.

2.2 Mechanical allodynia measurements

Animals were placed in clear, plastic, bottomless cages over a wire mesh surface and acclimated for at least 30 min before the initiation of testing and for 1 hour prior to initiation of the experiment. Tactile thresholds were measured with a series of von Frey filaments (Bioseb) ranging from 2.44 to 4.31 (0.02–2.00 g) using the up-down method and starting at 3.61 filament [5]. The 50% probability of withdrawal threshold was recorded. Mechanical withdrawal thresholds were assessed before treatment (baseline or day 0) and at the specified time points after treatment.

2.3 Intrathecal delivery of AIBP or saline

Mice were anesthetized using 5% isoflurane in oxygen for induction and 2% isoflurane in oxygen for maintenance of anesthesia. Intrathecal (i.t.) injections were performed according to Hylden and Wilcox et al., 1980 [14]. Briefly, the lower back was shaved and disinfected, and the animals were placed in a prone posture holding the pelvis between the thumb and forefinger. The L5 and L6 vertebrae were identified by palpation, and a 30G needle was inserted percutaneously into the midline between the L5 and L6 vertebrae. Successful entry was assessed by the observation of a tail flick. Injections of 5 μl were administered over an interval of 30 s, and the mouse then removed from anesthetic. Drugs for i.t. delivery were formulated in sterile 0.9% NaCl. Based on previous studies [31;40], AIBP dosing for spinal delivery in these studies was 0.5 μg/5 μl. Following recovery from anesthesia, mice were evaluated for normal motor coordination and muscle tone. The procedure and dosing did not cause motor dysfunction in any animals utilized for this study.

2.4 Analysis of lipid raft and TLR4 in DRG neurons by flow cytometry

Animals were euthanized on day 10 after the induction of CIPN model and DRGs from the lumbar region were collected to perform flow cytometry. Tissues were processed using a Neural Tissue Dissociation kit (Miltenyi Biotec) to reach single cell suspension. Debris Removal Solution kit (Miltenyi Biotec) was used to remove cell debris, following the manufacturer's protocol. To measure TLR4 dimerization in DRG neurons, cells were incubated with a mix of APC-Cy7 live/dead Ghost dye (Cell Signaling); cholera toxin B (CTxB)-Alexa594 (ThermoFisher-C34777); BV421-conjugated CD24 antibody (Biolegend), BV510-conjugated CD44 antibody (Biolegend), and BV650-conjugated CD45 antibody (Biolegend) to gate for neurons[42]; PE-conjugated TLR4/MD2 (MTS510) antibody ThermoFisher) and APC-conjugated total TLR4 (SA15–21) antibody (Biolegend), for 45 minutes on ice. After staining, cells were washed and analyzed using a CytoFLEX flow cytometer (Beckton Coulter). To calculate TLR4 dimers, the ratio of the geometric mean fluorescence intensity of PE-conjugated TLR4/MD2 (MTS510) antibody over APC-conjugated total TLR4 (SA15–21) antibody was calculated [31].

2.5 DRG culture

Male mice were euthanized under deep CO_2 anesthesia followed by decapitation. Thoracic and lumbar DRGs were harvested and transferred to Minimum Essential Medium Eagle solution (MEM, Gibco, #11095080). Ganglia were incubated in 0.125% collagenase type IV (Gibco, # 17104019) for 2 hours followed by incubation with 0.25% trypsin (Gibco, #25200056) for 6 min. Enzymatic dissociation steps were carried out at 36 °C. DRGs were washed three times with MEM and carefully dissociated, passing through a pipette using up and down movements (Linhart et al., 2003). A 10% BSA (Miltenyi Biotec #130-091-376) gradient was used to remove the debris from the tissue and separate a pellet of cells. The cells were resuspended and plated in glass bottom dishes coated with Poly-DL-ornithinehydrobromide (Sigma P8638) and maintained in DMEM containing penicillin and streptomycin (ThermoFisher, #15140122). Cultures were maintained in the incubator at 37°C with a 5% CO_2 atmosphere for 24 hours.

2.5.1 Calcium imaging of DRG neurons—All calcium imaging experiments were performed on intact DRG neurons plated on glass coverslips with a Poly-DL-ornithinehydrobromide substrate after 24h of DRG dissociation. DRG cell cultures were loaded with the Ca^{2+} indicator Fluo-4 AM (5 μM; Invitrogen. #F23917) in the presence of 2 mM probenecid for 30 min at 37°C in a HEPES-buffered saline (in mM): NaCl 122; KCl 3.3; CaCl2 1.3; MgSO4 0.4; KH2PO4 1.2; HEPES 25; glucose 10; adjusted with NaOH to pH 7.4. Coverslips were placed in a laminar flow perfusion chamber (Warner Instrument Corp., UK) and perfused with extracellular solution (in mM: NaCl 160; KCl 2.5; CaCl2 1; MgCl2 2; HEPES 10; glucose 10; pH 7.4) continuously via a perfusion system. The perfusion system consisted of three individual compartments, filled with treatment solutions, each one connected to a separate cannula that merged to one output cannula. The latter was inserted in the laminar flow perfusion chamber containing a glass coverslip with DRGs neurons. The flow occurred constantly, bathing the cells; each treatment valve was opened manually by the experimenter. A suction pump connected to outflow side of the chamber served to maintain a continuous perfusion. Experiments were performed at room temperature. DRG neurons were recorded in an inverted Leica TCS SP5 confocal microscope. One field of view per coverslip was assessed. Neurons were exposed to buffered vehicle for 2 min, then stimulated for 15 seconds with capsaicin (0.5 μM), then buffered for 4 minutes and finally stimulated with KCl (50 mM) for 5 seconds to confirm cellular viability. Neuronal Ca^{2+} responses were analyzed in 3–5 dishes from each culture by selecting individual cells as ROIs (Region of Interest) and calculating mean gray value variations on each individual cell using LAS AF version 2.7.3.9723 software. Data are presented as ΔF/F0, where F0 is the baseline, and the effect is quantified as maximal ΔF/F0.

2.5.1.1 Calcium evoked influx of DRG neurons acutely treated in vitro with paclitaxel: Before the calcium imaging experiment, DRG neurons from C57BL/6 naïve male mice were incubated with paclitaxel (3 μM) or vehicle (PBS), AIBP alone (1 μg/mL), or co-incubated with paclitaxel and AIBP for two hours at 37 °C. Cells were then loaded with Fluo-4 and evoked calcium images were recorded as described above.

2.5.1.2 Calcium evoked influx of DRG neurons obtained from CIPN mice: Male mice were i.p. injected with paclitaxel (2 injections of 8 mg/kg on days 1 and 3) or naïve mice, followed on day 7 by i.t. saline (5μl) or i.t. AIBP (0.5μg/5μl). Animals were euthanized on day 10 (3 days after i.t. injections), and thoracic and lumbar DRGs were collected for digestion and cell culture. Cells were plated on coverslips for 24 h prior to loading with Fluo-4 and evoked calcium imaging undertaken as described above.

2.5.2 MTT viability assay—DRG neurons were isolated from DRGs collected from naïve male mice and plated for 24h. Cells were incubated *in vitro* with paclitaxel (3 μM), AIBP alone (0.1 μg/mL, 0.5 μg/mL, or 1 μg/mL), or co-incubated with paclitaxel and AIBP for two hours. According to manufacturer instructions (abcam-Ab211091 – MTT Cell Proliferation Assay Kit), media were removed, and cells were incubated at 37°C with MTT reagent for 3 hours. After MTT solvent was added to the cells, the plate was incubated for 15 min under agitation, protected from light and read the absorbance at 590 nm.

2.3.5 Immunohistochemistry in cultured DRG neurons—DRG neurons, pre-treated or not with AIBP (0.2 μg/mL) for 30 min, were stimulated with LPS (100 ng/mL) for 15 min and then fixed with 4% PFA. Cells were blocked using fetal bovine serum (FBS) without permeabilization agents for 30 minutes and incubated with an anti-TLR4 antibody (Abcam, Ab22048, 1:100) and CTxB-Alexa555 conjugate (ThermoFisher, C34776, 1:250) for 2 hours. After washes, DRG neurons were incubated with secondary goat anti-mouse Alexa488 antibody (ThermoFisher, A28175, 1:1000) for 2 hours. Coverslips with cells were mounted in slides with ProlongGold containing DAPI and imaged using a Leica SP8 microscope. Fluorescence intensity and co-localization were analyzed in ImageJ.

2.6. Whole-mount DRG staining and imaging

Three days after intrathecal administration of AIBP (0.5μg/5μl), mice were euthanized and intracardially perfused with 0.9% NaCl solution followed by 4% PFA. Lumbar DRGs (L3–L5) were dissected out, post-fixed for 12 hours, and then stored in PBS with 0.02% sodium azide.

Whole DRGs were permeabilized in PBS, TritonX-100, glycine, and DMSO solution for two hours, blocked using FBS for 2 hours, and incubated with an anti-TRPV1 antibody (Novus Biologicals, NBP1–97417, 1:500) and CTxB-Alexa594 conjugate (ThermoFisher, C34777, 1:250) for 72 hours. After washes, DRGs were incubated with an anti-rabbit Alexa647 antibody (cell Signaling - 4414, 1:500) for 72 hours. After staining, DRGs were cleared, as described[13]. In brief, DRGs were dehydrated in tetrahydrofuran (THF)/H_2O series: 50%, 70%, 80%, 100% for 15 minutes each at room temperature on a shaker plate, then transferred to successive solutions of 66% dichloromethane (DCM)/ 33% THF and 100% DCM for 15 minutes each at room temperature on a shaker plate, followed by a 100% solution of dibenzyl ether (DBE) for clearing. DRGs were then transferred into imaging chambers mounted on glass slides. Imaging chambers were designed in-house to be 300 μm high and fit a 22 × 30 mm coverslip with a leakproof seal. A Z-stack of optical sections at 0.30 μm increment was captured using a 63x objective on a Leica SP8 confocal microscope.

2.6.2 Proximity ligation assay in whole-mount DRGs—To perform the PLA assay, DuoLink PLA Multicolor Reagent Pack (Sigma-Aldrich) was used along with DuoLink PLA Multicolor Promaker Kit-Orange to conjugate TRPV1 and CTB antibodies to oligo probes (for detection of TRPV1-CTxB proximity) and DuoLink PLA Multicolor Promaker Kit-Far Red to conjugate TRPV1 and TLR4 antibodies (for detection of TRPV1-TLR4 proximity), according to manufacturer's protocol. Whole DRGs were blocked for 2 hours before unconjugated CTxB was added for a 24-hour incubation. After washing, probe conjugated anti-TRPV1, anti-CTxB, and anti-TLR4 antibodies were added in a dilution of 1:100 to DRGs for 72 hours. Samples were washed, ligated for 6 hours, amplified overnight at 37°C, followed by an incubation with detection buffer for 6 hours. DRGs were washed and incubated with DAPI overnight. All incubation steps were performed at 37°C with agitation and protected from light. After completing the PLA protocol, DRGs were cleared as described above, transferred into imaging chambers and imaged using a 63x objective on a Leica SP8 confocal microscope. The same microscope settings were maintained consistent during scanning of DRGs across all groups. Two fields per each DRG were selected, one with high number of neuronal cell bodies and another with fewer neurons.

2.6.2.1 Image analysis of whole-mount DRG: Z-stack images of 4 DRGs per treatment group were imported to IMARIS 9.8.2 software, and surfaces were created to identify cell types and labelling for each channel. After surfaces were created, analysis of fluorescence intensity per voxel in the surfaces, the volume of each surface, and overlap with other surface/channels of interest were generated. Colocalization analysis in IMARIS was performed to calculate Pearson's coefficient between surfaces of interest (TRPV1 and CTB, or TRPV1-CTB PLA and TRPV1-TRL4 PLA).

2.7. Analysis of TRPV1 phosphorylation

DRGs from animals treated with paclitaxel and AIBP were collected and washed in cold Ca^{2+} and Mg^{2+}-free Hank's balanced salt solution, followed by homogenization in 0.2 ml RIPA buffer containing protease inhibitors (Cell Signaling Technology, 5872), and centrifugation at 13,000g for 20 min at 4°C to remove debris. Tissue lysates were heated in a sample buffer and loaded onto a 4–12% Bis-Tris NuPAGE gel (Invitrogen) at 10 μg/well, followed by transfer to a PVDF membrane. The blots were blocked and probed with antibodies against phospho-TRPV1 S502 (ThermoFisher PA5-64860) or total TRPV1 (Novus Biologicals, NBP1–97417), followed by an anti-rabbit IgG-HRP conjugated antibody (1:3,000). After washes, SuperSignal West Pico PLUS Chemiluminescent Substrate (ThermoFisher, 34580) was added to membranes for detection of protein bands, the blots were scanned using a UVP BioSpectrum imaging system and analyzed in ImageJ.

2.8 Nociceptive response to capsaicin *in vivo*

Naïve mice or the mice that treated with paclitaxel (2 i.p. injections of 8 mg/kg) on days 1 and 3, followed by i.t. saline (5μl) or i.t. AIBP (0.5μg/5μl) on day 7, received a single subcutaneous injection into central plantar region (right hind paw) of capsaicin (10 μg/25μL) on day 15. This paw area corresponds to the L5 DRG peripheral field. The mice were immediately placed on top of a wire mesh surface inside a clear bottomless cage, and the number of flinches (including flicking and licking) were recorded for 5 minutes by two

independent experimenters. Results were expressed as average of nociceptive response per group, considering the total number of flinches and licks, as previously described [18].

2.9 Data analysis

All results are presented as means ± SEM. The significance of differences between groups was established with unpaired t-test, one-way ANOVA, or two-way ANOVA followed by Tukey's test. A value of $P < 0.05$ was set as the threshold of statistical significance. Statistical analyses were performed in GraphPad Prism v9.2 (GraphPad Software). Group sizes were determined using power analyses based on prior behavior studies [31;40]. At least 2 independent cohort experiments were performed per analysis. To reduce selection bias and maintain rigor and reproducibility, randomization of animals after baseline measurements was performed for group treatment assignments across cages. The experimenter administering treatments and measuring behavioral responses was blinded to allocation of the treatments by a different experimenter using coded labeling.

3. Results

3.1. AIBP inhibits LPS-induced TLR4 localization to lipid rafts in DRG neurons

In immune cells, including macrophages and microglia, ligand-dependent TLR4 recruitment to lipid rafts is an initial step in the inflammatory cascade. Because DRG nociceptors express high levels of TLR4 [22], we tested the effect of LPS on lipid rafts and TLR4 in DRG neurons in culture. LPS induced a rapid increase in the level of lipid rafts and TLR4 recruitment to lipid rafts. Both of these effects were prevented by a pre-incubation with AIBP (Figure 1). Because TLR4 signaling has been implicated in DRG nociceptive responses [20–22], we hypothesized that TLR4 localization to lipid rafts might contribute to regulation of DRG neuronal excitability and that AIBP can control lipid raft-dependent processes in DRG neurons. To test these hypotheses *in vivo*, we used a mouse paclitaxel CIPN model.

3.2. Intrathecal AIBP alleviates CIPN tactile allodynia and controls TLR4-raft processes

In our prior studies, we demonstrated that a single i.t. injection of AIBP reversed established tactile allodynia in a cisplatin model of CIPN [31; 40]. Here, we demonstrated that in a paclitaxel CIPN model, i.t. AIBP also reversed established tactile allodynia (Figure 2A). The therapeutic effect of a single i.t. dose of AIBP in paclitaxel CIPN lasted for as long as five weeks (Supplementary Figure 1), which agrees with the long-lasting effect of AIBP in cisplatin CIPN [40]. In paclitaxel CIPN, we observed the reversal of mechanical allodynia by i.t. AIBP in both male and female mice (Supplementary Figure 1). The efficacy of a 0.5 μg dose of i.t. AIBP showed no significant differences between sexes. However, a tendency to observe a greater effect was noted in males as compared to females.

In the experiment shown in Figure 2A, animals were euthanized to collect the DRG tissue 3 days after i.t. AIBP. The L3–L6 DRGs were digested to obtain a single-cell suspension, and lipid rafts and TRL4 expression in neurons were analyzed by flow cytometry. We found that $CD45^{-}CD44^{-}CD24^{+}$ DRG neurons [42], which express TRPV1 (Supplementary Figure 2), isolated from paclitaxel/saline mice had significantly higher levels of lipid rafts and surface

TLR4 expression compared to those from naïve/saline mice. I.t. AIBP reversed both lipid rafts and TLR4 increases (Figure 2B and 2C). However, unlike in spinal microglia, we did not observe in the DRG neurons significant changes in TLR4 dimerization (Figure 2D). We hypothesized that in DRG neurons, TLR4 homodimerization was less prominent due to TLR4 interaction with other receptors.

Previous studies suggested that TLR4 can sensitize the TRPV1 ion channel, which significantly contributes to nociceptive signaling [19]. Thus, we measured TRPV1 localization to lipid rafts by assessing the signal of TRPV1 and its colocalization to lipid rafts signal (cholera toxin B, which binds the lipid raft component GM1 ganglioside). The TRPV1 staining in whole-mount DRGs demonstrated an increased TRPV1 localization to lipid rafts in paclitaxel/saline mice, which was reversed in the mice that received i.t. AIBP instead of saline (Figure 3). Further, the proximity between TRPV1 and TLR4, measured by PLA in DRG neurons, was also increased in paclitaxel CIPN mice and reversed by i.t. AIBP. Likewise, co-localization of TRPV1-TRL4 and TRPV1-lipid rafts pairs was increased in paclitaxel CIPN mice and reversed by i.t. AIBP. (Figure 4).

3.3 AIBP regulates TRPV1 sensitization in CIPN

To understand the functional implications of the displacement by AIBP of lipid raft TRPV1 and its reduced interaction with TLR4, we tested the nociceptive response to intraplantar capsaicin, a TRPV1 agonist, in naïve and CIPN mice treated with saline or AIBP. We observed that AIBP injection alone in naïve mice did not alter the nociceptive response to capsaicin. Paclitaxel induced an exaggerated nociceptive response to capsaicin. However, AIBP-treated paclitaxel mice displayed a nociceptive response similar to levels observed in naïve mice (Figure 5A). Phosphorylation of TRPV1 mediates its sensitization [3;15;25;33]. Accordingly, we observed increased phosphorylation of TRPV1 in the DRG tissue from mice treated with paclitaxel and lower phosphorylation levels of TRPV1 after AIBP treatment (Figure 5B). These results suggest that in addition to regulating lipid raft dynamics and TRPV1 proximity to TLR4 and rafts, AIBP desensitizes TRPV1 otherwise activated in CIPN.

To further evaluate the effect of AIBP on TRPV1, we measured capsaicin-induced changes in intracellular calcium concentration ($[Ca^{2+}]i$) in DRG neurons isolated from experimental groups. Neurons from animals that have developed CIPN after paclitaxel treatment were characterized by increased Ca^{2+} response to capsaicin, as compared to DRG neurons isolated from control mice. DRG neurons from animals that recovered from paclitaxel-induced CIPN after AIBP treatment had significantly lower Ca^{2+} responses to capsaicin compared to the neurons from CIPN only mice (Figure 5C).

We also tested Ca^{2+} response to capsaicin in DRG neurons from naïve mice treated *in vitro* with paclitaxel. We found that paclitaxel pre-treatment significantly increased Ca^{2+} influx in response to capsaicin compared to control. However, when DRG neurons were incubated with AIBP alone or with AIBP+paclitaxel, the Ca^{2+} response to capsaicin returned to the levels observed in control DRGs (Figure 6). These results support the conclusion that AIBP inhibits TRPV1 activity in DRG neurons. Interestingly, AIBP incubation also reduced calcium influx induced after KCl incubation (Supplementary Figure 3A and B). To confirm

that cells were still viable in the Figure 6 experiment, we performed an MTT assay and found that neither treatment affected DRG neurons viability (Supplementary Figure 3C). These results suggest that AIBP, via its effect on lipid rafts, may alter function of other ion channels in the membrane as well.

4. Discussion

This study provides new mechanistic insights into nociceptive signaling in DRG neurons and suggests a novel therapeutic approach to inhibit nociception and alleviate neuropathic pain in CIPN. Using a mouse model of CIPN, we demonstrated that administration of paclitaxel: increased lipid rafts, TLR4 expression and localization of TLR4 to rafts in DRG neurons and that these TLR4-rafts hosted TRPV1, facilitating the TRPV1-TLR4 interaction and TRPV1 phosphorylation. Intracellular calcium in response to the TRPV1 agonist capsaicin was increased in DRG neurons from paclitaxel treated mice and in the naïve mouse DRG neurons incubated i*n vitro* with paclitaxel. From the therapeutic perspective, i.t. AIBP, injected after tactile allodynia was established in paclitaxel treated mice, reversed all of the above characteristics of TRPV1 activation and alleviated the associated allodynia. AIBP also inhibited paclitaxel-augmented Ca^{2+} response to capsaicin in isolated DRG neurons.

We have previously shown that i.t. AIBP reduces spinal cord neuroinflammation in a model of cisplatin-induced CIPN [31;40]. We demonstrated that i.t. AIBP targeted TLR4 in microglia in these CIPN mice to reduce the facilitated pain behavior and expression of proinflammatory cytokines. However, TLR4 is expressed in other cell types, including small fiber nociceptors, which are critical in the development of CIPN [22]. Thus, we hypothesized that AIBP would target these neurons in neuropathy models induced by paclitaxel. The AIBP effects observed in the reversal of paclitaxel-induced allodynia and the molecular parameters evaluated in DRG neurons support the importance of TLR4 expression for mediating the AIBP effect. The results with paclitaxel and cisplatin induced CIPN also highlight the therapeutic potential of AIBP to target neuropathies induced by different classes of chemotherapeutic agents and possibly in other painful states where TLR4 has a pathophysiological role.

In microglia, AIBP targets TLR4-rafts (inflammarafts) by binding to TLR4, inducing cholesterol depletion from the plasma membrane. This cholesterol depletion results in dissociation of lipid rafts, preventing dimerization of TLR4 monomers and thereby inhibiting inflammatory signaling [31]. Like in microglia, *in vitro* LPS stimulation of DRG neurons resulted in a dramatic increase in lipid rafts and in TLR4 localization to lipid rafts. However, in contrast to spinal microglia under CIPN conditions, although DRG neurons displayed increased lipid rafts and TLR4 expression, TLR4-TLR4 dimers were not significantly increased compared to naive mice. We hypothesized that in DRG neurons, TLR4-rafts provide a platform not only for inflammatory signaling but also support TLR4 interaction with and facilitate the functionality of a *collection* of nociceptive receptors and channels co-expressed in the lipid raft. According to this hypothesis, the DRG neuronal TLR4-rafts would maintain voltage- and ligand-gated channels active in the lipid raft, preventing desensitization by internalization, or by increasing their activity via downstream TLR4 signaling. Here we show that in CIPN, TLR4 is found in close proximity to TRPV1

within the DRG neuronal lipid rafts and that this correlates with increased phosphorylation of TRPV1 in the DRG and with hyperalgesia when tested with intraplantar capsaicin. After treatment with AIBP, we observed that the TRPV1 lost its association with TLR4, was dislocated from the lipid raft, and showed reduced phosphorylation. These effects mirrored the reduced capsaicin-evoked calcium influx observed in *in vitro* and *in vivo* studies. These observations jointly support the conclusion that targeting TLR4-rafts in neurons can affect the functionality of receptors and/or channels associated with the TLR4 lipid rafts in DRG nociceptive neurons. This mechanism could explain the observed effect of TLR4 on sensitization of nociceptors via TRPV1 in pain reported previously [22;41], as well as enhanced TRPV1-mediated pruritus response [29], LPS-enhanced sensitization of TRPV1 in trigeminal sensory neurons [8], membrane-delimited excitatory actions via TRPA1 in neurogenic inflammation induced by LPS [26], and enhanced NMDA receptor-induced neuron excitability [4].

We demonstrate that in CIPN, TLR4 is found in close proximity to TRPV1 within the lipid rafts in DRG neurons and that this correlates with increased phosphorylation of TRPV1 in the DRG and with the behavioral assays assessing the respective roles of TRPV1 known to contribute to thermal and tactile hyperpathia following nerve injury. Although we did not examine changes in other behavioral endpoints mediated by TRPV1 including thermal hyperalgesia or pruritus, we directly demonstrated the effects of AIBP on TRPV1 activation through the paw focused pain behavior evoked by the intraplantar injection of capsaicin.

As AIBP binds to TLR4, it selectively targets the cholesterol depletion machinery towards TLR4 expressing cells. This serves to suppress activation of TLR4 expressing cells, with little adverse effect on cells not expressing TLR4 [10;27]. Indeed, i.t. AIBP had no effect on normal motor or non-nociceptive sensory function (light touch, proprioception) in normal mice [31]. Further, as AIBP treatment in naïve mice does not affect TRPV1 activity or nocifensive responses to capsaicin, does not it change lipid raft or TLR4 content in unconditioned DRG neurons, we propose that AIBP selectively targets activated TLR4-rafts, leaving intact normal cell functioning. In contrast to AIBP, other agents used to deplete cholesterol from the plasma membrane, such as cyclodextrins, apoA-I and its mimetic peptides, and LXR agonists, which upregulate the cholesterol transporters ABCA1 and ABCG1 expression, do not display any selectivity and are likely indiscriminate toward pathological and physiological lipid rafts. For example, cyclodextrin has only a transient effect on pain after repeated dosing and only when used as pre-treatment [23;40].

In vitro, AIBP inhibited not only capsaicin-induced changes in ($[Ca^{2+}]i$) but also those induced by KCl. We excluded the possibility of AIBP toxicity by testing neurons viability. This result indicates that the TLR4-raft may regulate the function of other receptors / channels that localize to these lipid rafts. Alternatively, AIBP effect could be indirect, via TRPV1-regulated sodium-calcium exchanger channels (NCX). Regulation of lipid rafts in neurons could target NCX inside rafts, which are activated once outside these domains [35], increasing the efficacy of Ca^{2+} extrusion after TRPV1-induced Ca^{2+} influxes via NCX. This may be a relevant mechanism given that spinal NCX has been recently reported as the locus for wind-up pain in humans [39].

Although this study focused on TLR4 clustering with TRPV1 in lipid rafts of DRG neurons, we do not exclude the possibility that TLR4-TRPV1 interactions can also occur in the terminals and/or in postsynaptic neurons in the spinal cord involved in pain signaling. As noted, other than TRPV1, TLR4-rafts may also host NCX, PIEZO1, Nav1.7 and Nav1.9 channels, and NMDA receptors, given that published studies suggest that TLR4 can interact with NMDAr [4;7] and Piezo1 [11], and that increased Nav1.7 and Nav1.9 current densities can occur via TLR4 activation [9]. Thus, future studies are likely to increase the repertoire of TLR4-raft partners that can be targeted by AIBP.

Supplementary Material

Refer to Web version on PubMed Central for supplementary material.

Acknowledgments

The authors thank Dr. Nicholas Webster for generously sharing access to a flow cytometer in his lab. This research was supported by NINDS grants NS102432 and NS104769 (to Miller and Yaksh), VA grants I01BX004848, IBX005224 (to Webster), NINDS NS047101 to UCSD Microscopy Core, and NIAMS grant AR075241 (to Gregus).

References

[1]. Amsalem M, Poilbout C, Ferracci G, Delmas P, Padilla F. Membrane cholesterol depletion as a trigger of Nav1.9 channel-mediated inflammatory pain. EMBO J 2018;37(8).

[2]. Aromolaran KA, Goldstein PA. Ion channels and neuronal hyperexcitability in chemotherapy-induced peripheral neuropathy; cause and effect? Mol Pain 2017;13:1744806917714693.

[3]. Assas BM, Miyan JA, Pennock JL. Cross-talk between neural and immune receptors provides a potential mechanism of homeostatic regulation in the gut mucosa. Mucosal Immunol 2014;7(6):1283–1289. [PubMed: 25183366]

[4]. Balosso S, Liu J, Bianchi ME, Vezzani A. Disulfide-containing high mobility group box-1 promotes N-methyl-D-aspartate receptor function and excitotoxicity by activating Toll-like receptor 4-dependent signaling in hippocampal neurons. Antioxidants & redox signaling 2014;21(12):1726–1740. [PubMed: 24094148]

[5]. Chaplan SR, Bach FW, Pogrel JW, Chung JM, Yaksh TL. Quantitative assessment of tactile allodynia in the rat paw. J Neurosci Methods 1994;53(1):55–63. [PubMed: 7990513]

[6]. Choi SH, Wallace AM, Schneider DA, Burg E, Kim J, Alekseeva E, Ubags ND, Cool CD, Fang L, Suratt BT, Miller YI. AIBP augments cholesterol efflux from alveolar macrophages to surfactant and reduces acute lung inflammation. JCI Insight 2018;3(16).

[7]. Cui J, Yu S, Li Y, Li P, Liu F. Direct binding of Toll-like receptor 4 to ionotropic glutamate receptor N-methyl-D-aspartate subunit 1 induced by lipopolysaccharide in microglial cells N9 and EOC 20. Int J Mol Med 2018;41(3):1323–1330. [PubMed: 29286078]

[8]. Diogenes A, Ferraz CC, Akopian AN, Henry MA, Hargreaves KM. LPS sensitizes TRPV1 via activation of TLR4 in trigeminal sensory neurons. J Dent Res 2011;90(6):759–764. [PubMed: 21393555]

[9]. Due MR, Piekarz AD, Wilson N, Feldman P, Ripsch MS, Chavez S, Yin H, Khanna R, White FA. Neuroexcitatory effects of morphine-3-glucuronide are dependent on Toll-like receptor 4 signaling. J Neuroinflammation 2012;9:200. [PubMed: 22898544]

[10]. Fang L, Miller YI. Regulation of lipid rafts, angiogenesis and inflammation by AIBP. Curr Opin Lipidol 2019;30(3):218–223. [PubMed: 30985364]

[11]. Geng J, Shi Y, Zhang J, Yang B, Wang P, Yuan W, Zhao H, Li J, Qin F, Hong L, Xie C, Deng X, Sun Y, Wu C, Chen L, Zhou D. TLR4 signalling via Piezo1 engages and enhances the macrophage mediated host response during bacterial infection. Nat Commun 2021;12(1):3519. [PubMed: 34112781]

[12]. Hara T, Chiba T, Abe K, Makabe A, Ikeno S, Kawakami K, Utsunomiya I, Hama T, Taguchi K. Effect of paclitaxel on transient receptor potential vanilloid 1 in rat dorsal root ganglion. Pain 2013;154(6):882–889. [PubMed: 23602343]

[13]. Hunt MA, Lund H, Delay L, Dos Santos GG, Pham A, Kurtovic Z, Telang A, Lee A, Parvathaneni A, Kussick E, Corr M, Yaksh TL. DRGquant: A new modular AI-based pipeline for 3D analysis of the DRG. J Neurosci Methods 2022;371:109497. [PubMed: 35181343]

[14]. Hylden JL, Wilcox GL. Intrathecal morphine in mice: a new technique. Eur J Pharmacol 1980;67(2–3):313–316. [PubMed: 6893963]

[15]. Joseph J, Qu L, Wang S, Kim M, Bennett D, Ro J, Caterina MJ, Chung MK. Phosphorylation of TRPV1 S801 Contributes to Modality-Specific Hyperalgesia in Mice. J Neurosci 2019;39(50):9954–9966. [PubMed: 31676602]

[16]. Kong W, Wang X, Yang X, Huang W, Han S, Yin J, Liu W, He X, Peng B. Activation of TRPV1 Contributes to Recurrent Febrile Seizures via Inhibiting the Microglial M2 Phenotype in the Immature Brain. Front Cell Neurosci 2019;13:442. [PubMed: 31680864]

[17]. Kovacs T, Sohajda T, Szente L, Nagy P, Panyi G, Varga Z, Zakany F. Cyclodextrins Exert a Ligand-like Current Inhibitory Effect on the KV1.3 Ion Channel Independent of Membrane Cholesterol Extraction. Front Mol Biosci 2021;8:735357. [PubMed: 34805269]

[18]. Lemes JBP, de Campos Lima T, Santos DO, Neves AF, de Oliveira FS, Parada CA, da Cruz Lotufo CM. Participation of satellite glial cells of the dorsal root ganglia in acute nociception. Neuroscience letters 2018;676:8–12. [PubMed: 29626652]

[19]. Li Y, Adamek P, Zhang H, Tatsui CE, Rhines LD, Mrozkova P, Li Q, Kosturakis AK, Cassidy RM, Harrison DS, Cata JP, Sapire K, Zhang H, Kennamer-Chapman RM, Jawad AB, Ghetti A, Yan J, Palecek J, Dougherty PM. The Cancer Chemotherapeutic Paclitaxel Increases Human and Rodent Sensory Neuron Responses to TRPV1 by Activation of TLR4. J Neurosci 2015;35(39):13487–13500. [PubMed: 26424893]

[20]. Li Y, Marri T, North RY, Rhodes HR, Uhelski ML, Tatsui CE, Rhines LD, Rao G, Corrales G, Abercrombie TJ, Johansson CA, Dougherty PM. Chemotherapy-induced peripheral neuropathy in a dish: dorsal root ganglion cells treated in vitro with paclitaxel show biochemical and physiological responses parallel to that seen in vivo. Pain 2021;162(1):84–96. [PubMed: 32694383]

[21]. Li Y, Tatsui CE, Rhines LD, North RY, Harrison DS, Cassidy RM, Johansson CA, Kosturakis AK, Edwards DD, Zhang H, Dougherty PM. Dorsal root ganglion neurons become hyperexcitable and increase expression of voltage-gated T-type calcium channels (Cav3.2) in paclitaxel-induced peripheral neuropathy. Pain 2017;158(3):417–429. [PubMed: 27902567]

[22]. Li Y, Zhang H, Zhang H, Kosturakis AK, Jawad AB, Dougherty PM. Toll-like receptor 4 signaling contributes to Paclitaxel-induced peripheral neuropathy. J Pain 2014;15(7):712–725. [PubMed: 24755282]

[23]. Lin CL, Chang CH, Chang YS, Lu SC, Hsieh YL. Treatment with methyl-beta-cyclodextrin prevents mechanical allodynia in resiniferatoxin neuropathy in a mouse model. Biol Open 2019;8(1).

[24]. Loprinzi CL, Lacchetti C, Bleeker J, Cavaletti G, Chauhan C, Hertz DL, Kelley MR, Lavino A, Lustberg MB, Paice JA, Schneider BP, Smith EML, Smith ML, Smith TJ, Wagner-Johnston N, Hershman DL. Prevention and Management of Chemotherapy-Induced Peripheral Neuropathy in Survivors of Adult Cancers: ASCO Guideline Update. J Clin Oncol 2020;38(28):3325–3348. [PubMed: 32663120]

[25]. Mandadi S, Armati PJ, Roufogalis BD. Protein kinase C modulation of thermo-sensitive transient receptor potential channels: Implications for pain signaling. J Nat Sci Biol Med 2011;2(1):13–25. [PubMed: 22470230]

[26]. Meseguer V, Alpizar YA, Luis E, Tajada S, Denlinger B, Fajardo O, Manenschijn JA, Fernandez-Pena C, Talavera A, Kichko T, Navia B, Sanchez A, Senaris R, Reeh P, Perez-Garcia MT, Lopez-Lopez JR, Voets T, Belmonte C, Talavera K, Viana F. TRPA1 channels mediate acute neurogenic inflammation and pain produced by bacterial endotoxins. Nat Commun 2014;5:3125. [PubMed: 24445575]

[27]. Miller YI, Navia-Pelaez JM, Corr M, Yaksh TL. Lipid rafts in glial cells: role in neuroinflammation and pain processing. J Lipid Res 2020;61(5):655–666. [PubMed: 31862695]

[28]. Min H, Cho WH, Lee H, Choi B, Kim YJ, Lee HK, Joo Y, Jung SJ, Choi SY, Lee S, Lee SJ. Association of TRPV1 and TLR4 through the TIR domain potentiates TRPV1 activity by blocking activation-induced desensitization. Mol Pain 2018;14:1744806918812636.

[29]. Min H, Lee H, Lim H, Jang YH, Chung SJ, Lee CJ, Lee SJ. TLR4 enhances histamine-mediated pruritus by potentiating TRPV1 activity. Mol Brain 2014;7:59. [PubMed: 25139109]

[30]. National Research Council (U.S.). Committee for the Update of the Guide for the Care and Use of Laboratory Animals., Institute for Laboratory Animal Research (U.S.), National Academies Press (U.S.). Guide for the care and use of laboratory animals. Washington, D.C.: National Academies Press,, 2011. pp. xxv, 220 p.

[31]. Navia-Pelaez JM, Choi SH, Dos Santos Aggum Capettini L, Xia Y, Gonen A, Agatisa-Boyle C, Delay L, Goncalves Dos Santos G, Catroli GF, Kim J, Lu JW, Saylor B, Winkels H, Durant CP, Ghosheh Y, Beaton G, Ley K, Kufareva I, Corr M, Yaksh TL, Miller YI. Normalization of cholesterol metabolism in spinal microglia alleviates neuropathic pain. J Exp Med 2021;218(7):e20202059. [PubMed: 33970188]

[32]. Park HJ, Stokes JA, Corr M, Yaksh TL. Toll-like receptor signaling regulates cisplatin-induced mechanical allodynia in mice. Cancer Chemother Pharmacol 2014;73(1):25–34. [PubMed: 24162377]

[33]. Premkumar LS, Ahern GP. Induction of vanilloid receptor channel activity by protein kinase C. Nature 2000;408(6815):985–990. [PubMed: 11140687]

[34]. Saghy E, Szoke E, Payrits M, Helyes Z, Borzsei R, Erostyak J, Janosi TZ, Setalo G Jr., Szolcsanyi J. Evidence for the role of lipid rafts and sphingomyelin in Ca2+-gating of Transient Receptor Potential channels in trigeminal sensory neurons and peripheral nerve terminals. Pharmacol Res 2015;100:101–116. [PubMed: 26238178]

[35]. Sibarov DA, Poguzhelskaya EE, Antonov SM. Downregulation of calcium-dependent NMDA receptor desensitization by sodium-calcium exchangers: a role of membrane cholesterol. BMC Neurosci 2018;19(1):73. [PubMed: 30419823]

[36]. Somdatta Saha AG, Tiwari Nikhil, Kumar Ashutosh, Kumar Abhishek & Goswami Chandan. Preferential selection of Arginine at the lipid-water-interface of TRPV1 during vertebrate evolution correlates with its snorkeling behaviour and cholesterol interaction. Sci Rep 2017.

[37]. Startek JB, Talavera K. Lipid Raft Destabilization Impairs Mouse TRPA1 Responses to Cold and Bacterial Lipopolysaccharides. Int J Mol Sci 2020;21(11).

[38]. Szoke E, Borzsei R, Toth DM, Lengl O, Helyes Z, Sandor Z, Szolcsanyi J. Effect of lipid raft disruption on TRPV1 receptor activation of trigeminal sensory neurons and transfected cell line. Eur J Pharmacol 2010;628(1–3):67–74. [PubMed: 19958765]

[39]. Trendafilova T, Adhikari K, Schmid AB, Patel R, Polgar E, Chisholm KI, Middleton SJ, Boyle K, Dickie AC, Semizoglou E, Perez-Sanchez J, Bell AM, Ramirez-Aristeguieta LM, Khoury S, Ivanov A, Wildner H, Ferris E, Chacon-Duque JC, Sokolow S, Saad Boghdady MA, Herchuelz A, Faux P, Poletti G, Gallo C, Rothhammer F, Bedoya G, Zeilhofer HU, Diatchenko L, McMahon SB, Todd AJ, Dickenson AH, Ruiz-Linares A, Bennett DL. Sodium-calcium exchanger-3 regulates pain “wind-up”: From human psychophysics to spinal mechanisms. Neuron 2022.

[40]. Woller SA, Choi SH, An EJ, Low H, Schneider DA, Ramachandran R, Kim J, Bae YS, Sviridov D, Corr M, Yaksh TL, Miller YI. Inhibition of Neuroinflammation by AIBP: Spinal Effects upon Facilitated Pain States. Cell reports 2018;23(9):2667–2677. [PubMed: 29847797]

[41]. Wu Y, Wang Y, Wang J, Fan Q, Zhu J, Yang L, Rong W. TLR4 mediates upregulation and sensitization of TRPV1 in primary afferent neurons in 2,4,6-trinitrobenzene sulfate-induced colitis. Mol Pain 2019;15:1744806919830018.

[42]. Yuan SH, Martin J, Elia J, Flippin J, Paramban RI, Hefferan MP, Vidal JG, Mu Y, Killian RL, Israel MA, Emre N, Marsala S, Marsala M, Gage FH, Goldstein LS, Carson CT. Cell-surface marker signatures for the isolation of neural stem cells, glia and neurons derived from human pluripotent stem cells. PLoS One 2011;6(3):e17540. [PubMed: 21407814]

[43]. Zhang H, Dougherty PM. Enhanced excitability of primary sensory neurons and altered gene expression of neuronal ion channels in dorsal root ganglion in paclitaxel-induced peripheral neuropathy. Anesthesiology 2014;120(6):1463–1475. [PubMed: 24534904]

[44]. Zhang M, Li L, Xie W, Wu JF, Yao F, Tan YL, Xia XD, Liu XY, Liu D, Lan G, Zeng MY, Gong D, Cheng HP, Huang C, Zhao ZW, Zheng XL, Tang CK. Apolipoprotein A-1 binding protein promotes macrophage cholesterol efflux by facilitating apolipoprotein A-1 binding to ABCA1 and preventing ABCA1 degradation. Atherosclerosis 2016;248:149–159. [PubMed: 27017521]

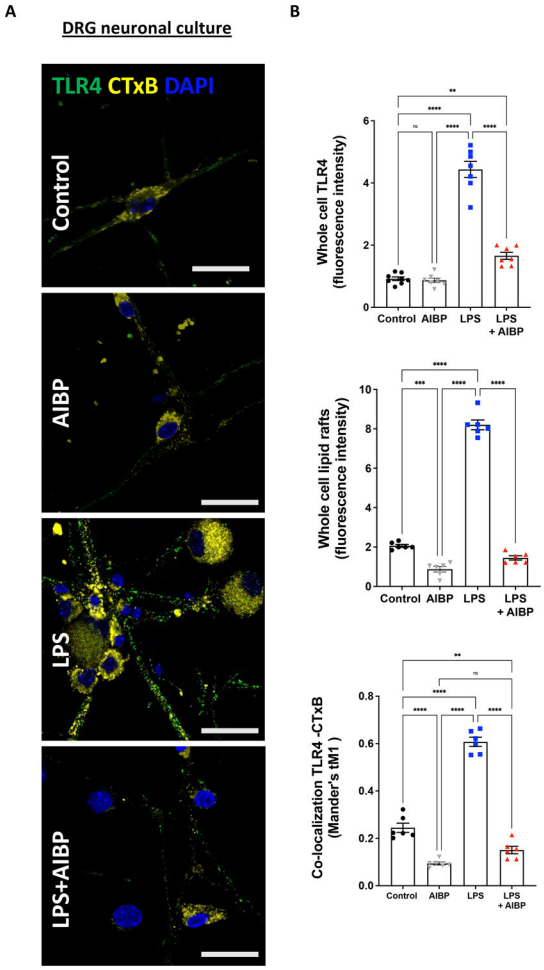

Figure 1: AIBP regulates TLR4 and lipid raft dynamics in response to LPS in DRG neurons in vitro.

A. DRG neurons from wild-type mice were cultured and stimulated with 100 ng/mL LPS for 15 min or pre–treated with AIBP (0.2 μg/mL) for 30 min and then incubated with LPS for 15 min and probed for lipid rafts (CTxB, binds the lipid raft component GM1 ganglioside; yellow) and TLR4 expression (green). Scale bar, 20 μm. **B**. Quantified fluorescence intensity of TLR4 and CTxB (lipid rafts), and colocalization of TLR4 and CTxB (lipid rafts) puncta. Mean±SEM; n=6. 2 dishes of cultured neurons from 3 different animals were stimulated in vitro. *, $p<0.05$; **, $p<0.01$ (one-way ANOVA).

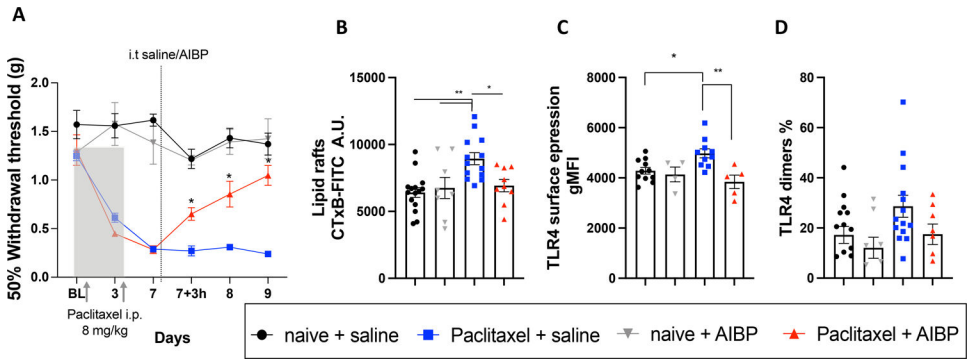

Figure 2: Intrathecal AIBP reverses paclitaxel-induced allodynia and alters lipid rafts and TLR4 expression in DRG neurons.

A. Hindpaw withdrawal thresholds in male mice in response to i.p. paclitaxel (2 injections of 8 mg/kg), followed by a single dose of i.t. saline (5 μl) or AIBP (0.5 μg/ 5 μl). Naïve mice received no i.p. injections (n=5–14 per group). Data shown from 2 independent experiments. **B-D.** Mouse groups shown in A were terminated on day 10, i.e, 72 hours after i.t. saline or AIBP, and DRG single-cell suspensions were analyzed by flow cytometry. Neurons were gated as $CD45^{-}/CD44^{-}/CD24^{+}$ cells and analyzed for lipid raft content, measured by CTxB (lipid rafts) staining (B), total surface TLR4 (C); and dimerized TLR4 (D). Data shown from 2 independent experiments. Mean±SEM; *, $p<0.05$; **, $p<0.01$ (two-way (A) and one way (B-D) ANOVA).

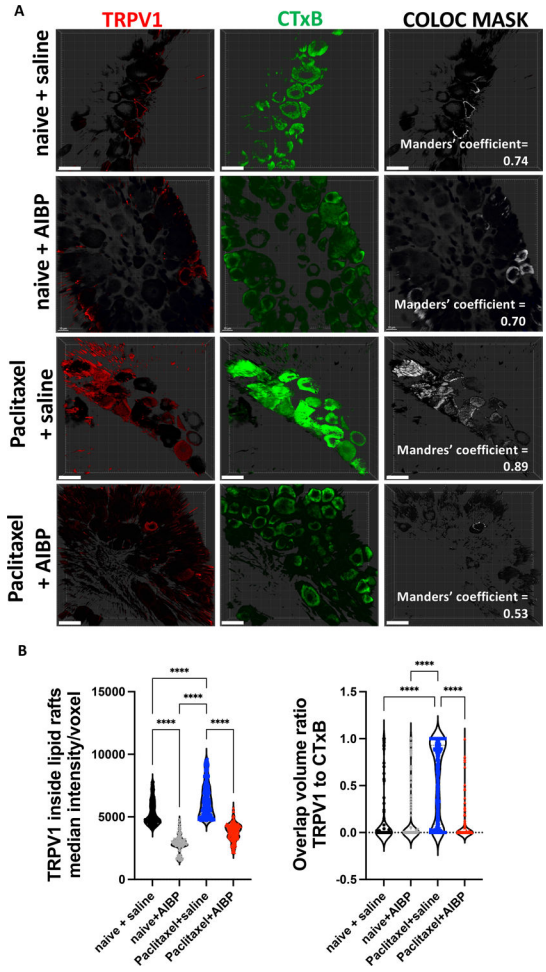

Figure 3: CIPN increases lipid raft content and TRPV1 localization to lipid rafts in DRG neurons.

A-B. Whole DRGs were collected from male mice treated with to i.p. paclitaxel (2 injections of 8 mg/kg), followed by i.t. saline (5µl) or AIBP (0.5 µg/ 5 µl), as in Fig. 2A (but in a separate experiment), stained for TRPV1 (red), and lipid rafts (CTxB; green), and subjected to a clearing protocol as described in Methods. Representative images (A) and quantitative data (B). Scale bar, 20 µm. Mean±SEM (n=4 per group); ****, $p<0.0001$ (one-way ANOVA).

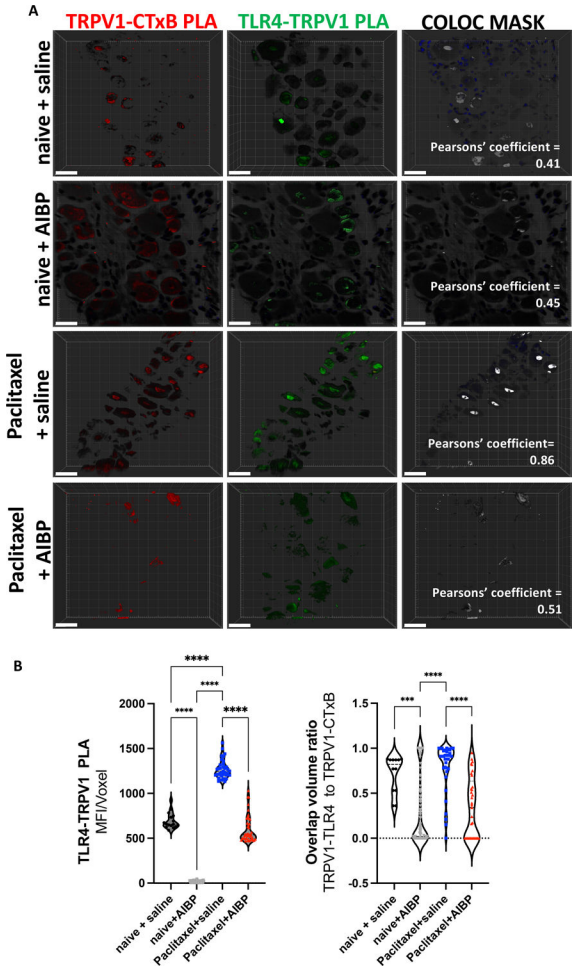

Figure 4: CIPN increases TLR4-TRPV1 interaction localization to lipid rafts.

A-B. Whole DRGs collected from experimental groups shown in Fig. 3 were subjected to a PLA protocol as described in Methods to detect proximity of TLR4-TRPV1 and TRPV1-CTxB (lipid rafts) in the same specimens. Representative images (A) and quantitative data for intensity/voxel and colocalization (B). Scale bar, 20 μm. Mean±SEM (n=4 per group); ****, p<0.0001 (one-way ANOVA).

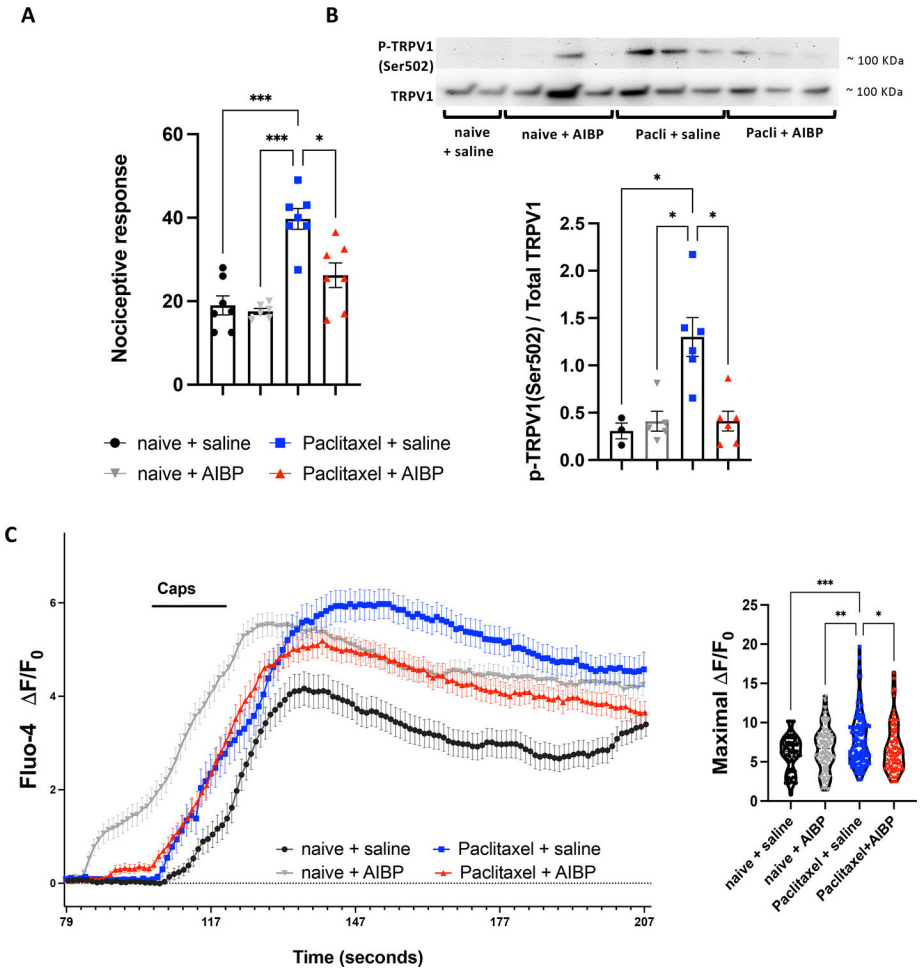

Figure 5: CIPN increases activation of TRPV1: reversal by AIBP.

A. Mice treated with i.p. paclitaxel (2 injections of 8 mg/kg) or naive, followed on day 7 by i.t. saline (5 μl) or AIBP (0.5 μg/ 5 μl), received on day 15 an intraplantar injection of capsaicin (10 μg/ 25μL), and the number of flinches over a 5 min period were recorded. n=6–7 **B.** Phosphorylation of TRPV1 (Ser502) was measured by western blot in DRG tissue from experimental groups shown in Fig. 2A (n=5–6). **C.** Calcium influx in response to capsaicin was recorded from DRG neurons isolated on day 10 from mice treated with i.p. paclitaxel (2 injections of 8 mg/kg) or naive, followed on day 7 by i.t. saline (5 μl) or AIBP (0.5 μg/ 5 μl), and loaded with Fluo-4. Neurons were buffered for 2 min, then stimulated for 15 sec with capsaicin (0.5 μM). The maximal $\Delta F/F_0$ was quantified for the capsaicin response. For analysis 5–9 neuron culture dishes from 4 different in vivo treated animals were used. Total number of recorded cells per treatments: naive+saline=74, naive+AIBP=122, paclitaxel+saline=97, and paclitaxel+AIBP=118. The earlier timepoint for calcium response in the AIBP group is due to a technical issue of using an experimental setup equipped with manually operated valves. Mean±SEM; *, p<0.05; ***, p<0.001; ****, p<0.0001 (one-way ANOVA).

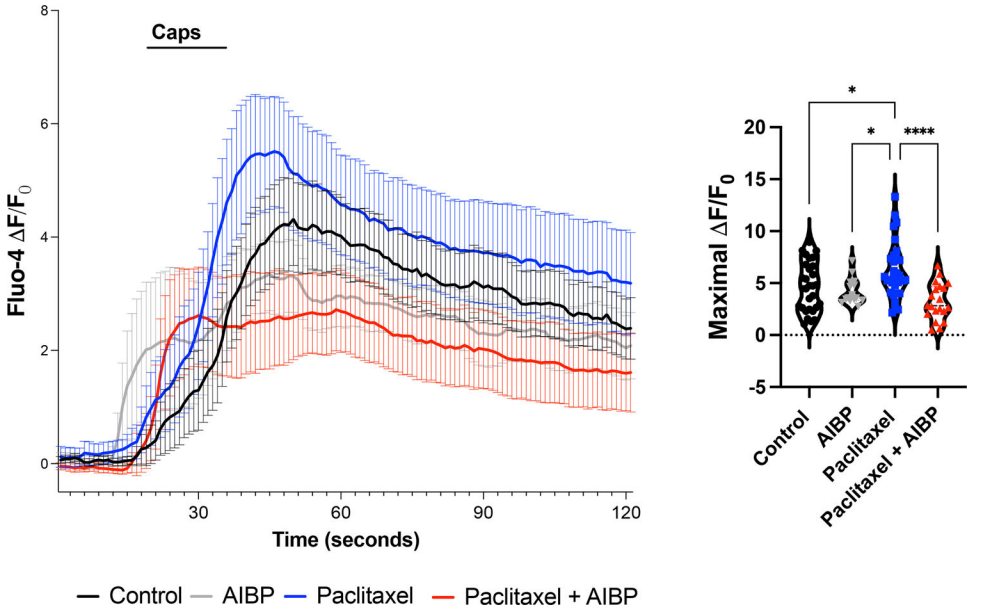

Figure 6: Paclitaxel increases TRPV1 activity in vitro: inhibition by AIBP.

Calcium influx in response to capsaicin was recorded from DRG cultured neurons incubated for 2 hours with paclitaxel (3 μM), AIBP 0.1 μg/mL, or paclitaxel+AIBP, and then loaded with Fluo-4. Neurons were buffered for 2 min, then stimulated for 15 sec with capsaicin (0.5 μM). See Supplemental Figure 3 for subsequent KCl stimulation. The maximal $\Delta F/F_0$ was quantified for the capsaicin response. Five to nine neuronal culture dishes from 4 different naïve wild type mice were stimulated in vitro. Total number of recorded cells per treatments: control(buffer)=19, paclitaxel=23, AIBP=15, and paclitaxel+AIBP=20. Mean±SEM; **, $p<0.01$. ***, $p<0.001$ (one-way ANOVA).